

Density Distribution in a Hard-Sphere Crystal.

R. OHNESORGE, H. LÖWEN and H. WAGNER

*Sektion Physik der Universität München
Theresienstraße 37, D-8000 München 2, Germany*

(received 3 December 1992; accepted in final form 12 March 1993)

PACS. 61.50 – Crystalline state (inc. molecular motions in solids).

PACS. 05.20 – Statistical mechanics.

PACS. 61.20J – Computer simulation of static and dynamic behaviour.

Abstract. – We performed extensive Monte Carlo simulations of a hard-sphere f.c.c. crystal near the melting transition in order to examine the validity of the widely used Gaussian ansatz for the density distribution in solids. Anisotropic deviations in the shape of the density distribution from the Gaussian form are found to be of the order of 10%. Popular liquid-based density functional approximations are shown to fail in predicting the magnitude and the qualitative features of the anisotropy in the crystalline density distributions.

Computer simulations [1] have revealed that the hard-sphere fluid freezes into a dense-packed crystal which is stabilized only by entropy and is thus entirely anharmonic. This phase transition occurs with coexisting densities $\rho_l \sigma^3 = 0.944$ and $\rho_s \sigma^3 = 1.04$, with σ denoting the hard-sphere diameter. In the current density functional theory of the freezing of simple liquids with a strongly repulsive core potential, hard spheres are normally employed as a suitable reference system. The short-range order, governed by the repulsive core, is thereby carried over to the solid phase and freezing is viewed as a condensation of density waves (see [2] for a recent review). In this variational approach, the free energy is expressed as a functional of the single-particle density which becomes minimal for the equilibrium distribution $\rho(\mathbf{r})$. In the solid phase, the lattice-periodic $\rho(\mathbf{r})$ also reflects the anisotropic point group symmetry of the crystal. However, in practical calculations, the density distribution is often taken to be a superposition of isotropic Gaussians centred at the lattice sites $\{\mathbf{R}\}$,

$$\rho^{(G)}(\mathbf{r}) = \left(\frac{\alpha}{\pi}\right)^{3/2} \sum_{\mathbf{R}} \exp[-\alpha(\mathbf{r} - \mathbf{R})^2], \quad (1)$$

where α is a variational parameter for the width of the peaks.

In this letter, we examine the validity of the ansatz (1) for a hard-sphere crystal near melting where deviations from the Gaussian approximation should be most pronounced. For this purpose, we present Monte Carlo (MC) results for density profiles in [100], [110] and [111] directions from an f.c.c. lattice position. The MC profiles are then compared with those obtained from density functional theory within the weighted-density approximation (WDA) [3] and its simplified version (MWDA) [4], in particular.

As a measure for the width of a lattice peak in $\rho(r)$ we consider the Lindemann parameter L [5], which relates the root-mean-square displacement to the nearest-neighbour distance a_{nn} :

$$L = \sqrt{\int_{\text{WSC}} d^3r r^2 \rho(r)} / a_{nn} \quad (2)$$

with integration over a Wigner-Seitz cell (WSC) centred at the origin. The anisotropy of the peak density will be characterized by the ratio Δ of displacements in two different directions e_1 and e_2 ,

$$\Delta(e_1, e_2) = \frac{\int dx \rho(xe_1) x^4}{\int dx \rho(xe_2) x^4}. \quad (3)$$

Here the one-dimensional integration extends from the origin to the WSC boundary.

In our Monte Carlo work, we have simulated an f.c.c. solid consisting of $N = 16384$ hard spheres in a periodically repeated cubic box and evaluated $5 \cdot 10^4$ Monte Carlo steps per particle. We chose the solid mean density $\rho_0 = 1.0409\sigma^{-3}$ at solid-liquid coexistence [1]. During the simulation, it was checked that the particles do not escape from their nearest-neighbour cages. The results for $\rho(r)r^2$, with r denoting the distance from the lattice site, are displayed in fig. 1a). The anisotropy becomes visible only for $r > 0.15\sigma$, and is most pronounced in the tails. The density distribution is broadest in the [100] direction as one would expect intuitively since in this case the hard spheres have more space available than in the directions towards their nearest neighbours. The profiles in the [111] and [110] directions practically coincide. We have also made an isotropic Gaussian least-square fit, $\rho^{(G)}(r)$, to the Monte Carlo data; the results for $\Delta\rho(r)r^2 = (\rho(r) - \rho^{(G)}(r))r^2$ are shown in fig. 1b). The deviation is negligible in the vicinity of the lattice site, but becomes more distinctive for larger particle displacements r . This implies that the ansatz (1) is indeed a reasonable global approximation, but details in the wings of the distribution show a marked deviation from the Gaussian behaviour.

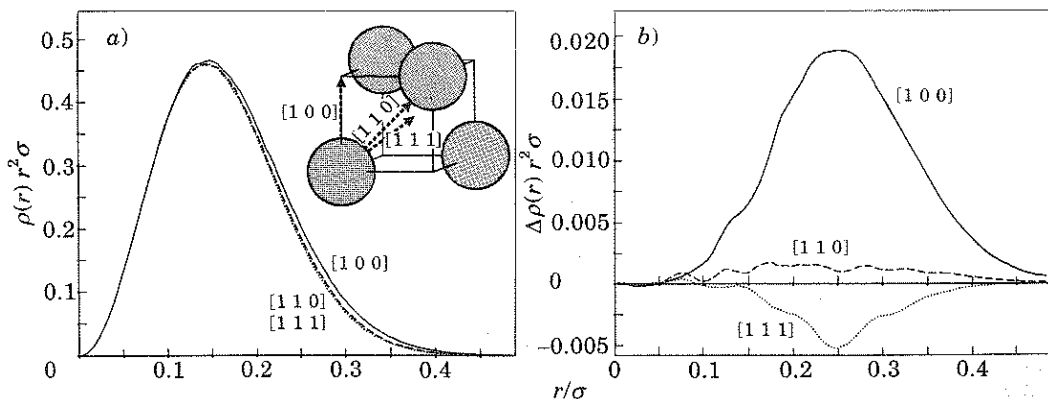


Fig. 1. - Density distribution near a lattice site of a hard-sphere solid with mean density $\rho_0 = 1.0409\sigma^{-3}$ calculated by Monte Carlo simulation. In a) $\rho(r)r^2$ is shown along the three directions indicated in the inset: [100] (solid line), [110] (dashed line), [111] (dotted line). In b) a Gaussian has been subtracted from the curves in a). The wiggles in the curves in b) are due to the statistical error of the simulation.

TABLE I. - Comparison of the Lindemann parameter L and the anisotropy parameter Δ calculated by computer simulation and density functional theory. The simulation data are given for two different densities. The density functional calculations have been done for two functionals, each one minimized freely, and in the subspace of Gaussians.

Method	$\rho_0 \sigma^{-3}$	L	$\Delta([100], [110])$	$\Delta([100], [111])$
Monte Carlo	1.0409	0.129	1.086	1.113
Monte Carlo	1.3000	0.0309	1.037	1.044
MWDA, Gaussians	1.0409	0.0979	1.000	1.000
MWDA, free minimum	1.0409	0.128	0.63	0.15
WDA, Gaussians	1.0409	0.0973	1.000	1.000
WDA, free minimum	1.0409	0.121	0.61	0.40

In order to determine the Lindemann parameter L and the anisotropy parameter Δ , one must correct for finite-size effects. The results obtained with data from smaller systems and after scaling linear in $N^{-1/3}$ are given in the first line of table I. The maximum anisotropy is at most about 11 percent. We have also simulated an f.c.c. crystal with the higher density $\rho_0 = 1.3\sigma^{-3}$. As expected, the anisotropy is less pronounced but has the same directional signature. The results are also included in table I. Simulations of the density distribution in hard-sphere crystals have been carried out earlier [6] but, at that time, the statistical errors were too large to allow for reliable inferences on the detailed anisotropic structure of $\rho(r)$.

Density functional approximations such as the WDA or the computationally simpler MWDA yield reasonably accurate phase diagrams for the hard-sphere fluid. Here, we examine whether these methods are also able to reproduce more subtle structural features as, for instance, the anisotropy of the crystalline single-particle distribution⁽¹⁾. This problem has been addressed recently by Laird *et al.* [8] within the Ramakrishnan-Yussouff approach [9].

In MWDA [4], the Helmholtz free energy of the system is given by

$$\mathcal{F}^{\text{MWDA}}[\rho] = \mathcal{F}^{\text{ideal}}[\rho] + \rho_0 V \psi(\bar{\rho}). \tag{4}$$

$\mathcal{F}^{\text{ideal}}$ denotes the exactly known ideal-gas contribution, ρ_0 is the mean density, V the volume and ψ the excess free energy per particle of the homogeneous fluid. The strongly inhomogeneous crystal is mapped onto a liquid via the weighted density

$$\bar{\rho} = \frac{1}{\rho_0 V} \int d^3r \int d^3r' \rho(r) \rho(r') \bar{w}(|r - r'|; \bar{\rho}). \tag{5}$$

The weight function $w(r; \rho)$ is determined by requiring the functional $\mathcal{F}^{\text{MWDA}}[\rho]$ to reproduce the correct pair correlations of the homogeneous liquid. With $c^{(2)}(r; \rho_0)$ denoting the direct Ornstein-Zernike correlation function in a liquid of density ρ_0 , the weight function is then

⁽¹⁾ Alternative theoretical approaches to the hard-sphere solid density are cluster-cell or self-consistent field theories (see [7]) which start from the situation of closed-packing and are thus valid only for very high solid densities where the effects of anisotropy are rather small. These approaches have not yet been applied to study the effects of anisotropy at melting.

$$w(r; \rho_0) = \frac{-1}{2\psi'(\rho_0)} \left[k_B T c^{(2)}(r; \rho_0) + \psi''(\rho_0) \frac{\rho_0}{V} \right]. \quad (6)$$

We performed a virtually free minimization of $\mathcal{F}^{\text{MWDA}}[\rho]$ using the Fourier components $\rho(\mathbf{k})$ from about 40 000 k -shells in the reciprocal lattice as variational parameters. The minimization is constrained by requiring that each elementary cell is occupied by one particle. As for $c^{(2)}(r; \rho_0)$, we adopt the Percus-Yevick expression; the excess free energy $\psi(\rho_0)$ is then obtained from the compressibility relation. A simulated-annealing method, which has been applied successfully to inhomogeneous liquids [10], for instance, is then used to find the minimizing density in the high-dimensional parameter space.

The results for $\rho(r)r^2$ are shown in fig. 2 together with the Monte Carlo [100] profile. In comparison with the MC results, the density distribution in MWDA is more strongly localized at the lattice sites; moreover, the profile in the [110]-direction (pointing towards the nearest neighbour) now turns out to be the broadest. We also employed the WDA and found the same features. Thus, both approximations fail even qualitatively in their prediction of the anisotropy of $\rho(r)$ [11]. The values of L and Δ are given in table I. For comparison, we also included the corresponding data from a minimization in the subspace of Gaussian density distributions. As compared to the Lindemann parametrization, the free minimization yields significantly higher values for the Lindemann parameter which are in excellent agreement with the simulation data. A similar shift was found in ref. [12]. At first glance, this seems to be a real improvement over the Gaussian approximation. However, the enhancement of L is mainly due to an unphysical high interstitial density. This feature is illustrated by the inset of

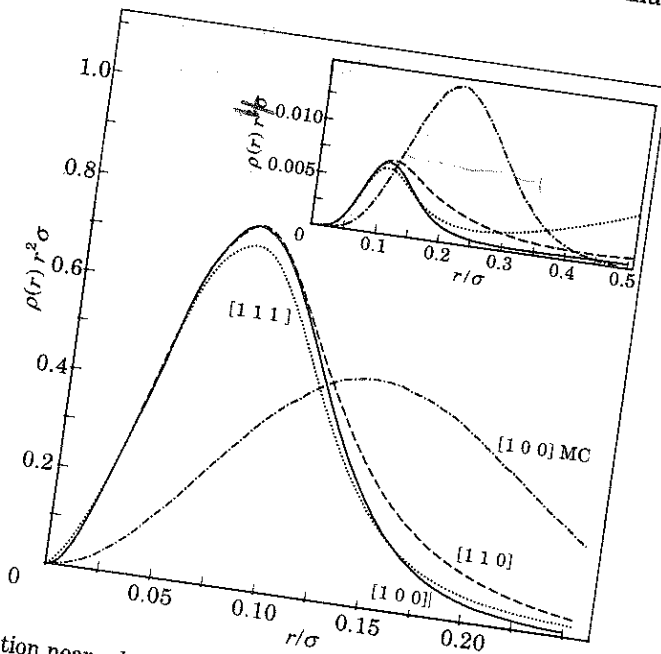


Fig. 2. - Density distribution near a lattice site of a hard-sphere solid with mean density $\rho_0 = 1.0409\sigma^{-3}$ calculated within the MWDA. $\rho(r)r^2$ is shown for three crystal directions, [100] (solid line), [110] (dashed line), [111] (dotted line). The Monte Carlo [100]-profile (dash-dotted line) is included for comparison. The inset shows $\rho(r)r^4$ for the same density distributions.

$9\sigma^{-3}$
n the
from
f the

fig. 2 where $\rho(r)r^4$ is shown which is the integrand of the second moment of an isotropic density distribution. While $\rho(r)$ decreases, this quantity is spread out in the interstitial region and thus contributes significantly to L .

To summarize: we calculated and discussed the density distribution in a hard-sphere solid near the melting point. The global form of the density distribution was found to be quite close to a Gaussian. However, the tails of the distribution show a significant anisotropy and non-Gaussian behaviour. The liquid-state-based density functional approximations such as WDA and MWDA predict the anisotropic features of the single-particle density distribution incorrectly.

We conclude with two comments: 1) it would be instructive to check the Monte Carlo predictions experimentally with real hard spheres like probes. As a suitable material we suggest an index-matched nearly monodisperse sterically stabilized colloidal suspension where the interparticle interactions are completely governed by excluded-volume effects [13]. By using an external field produced by different laser beams one could in principle force the fluid suspension to freeze into a pure single f.c.c. crystal. After compressing the crystal and removing the stabilizing field, the real-space particle density may be examined by light microscopy. 2) The technique of free minimization is also applicable to other physically interesting situations such as solids in contact with walls, solid-liquid interfaces and surface melting, where effects due to anisotropy are presumably of minor importance. This method has already been applied to study strongly inhomogeneous density profiles of hard-sphere liquid mixtures near a rigid wall within a novel hybridized form of the weighted-density approximation [14].

We acknowledge helpful discussions with E.-J. MEIJER. This work was supported by the Bundesministerium für Forschung und Technologie (BMFT) under Contract No. 03WA2LMU.

REFERENCES

- [1] HOOVER W. G. and REE F., *J. Chem. Phys.*, **49** (1968) 3609.
- [2] SINGH Y., *Phys. Rep.*, **207** (1991) 351.
- [3] CURTIN W. A. and ASHCROFT N. W., *Phys. Rev. A*, **32** (1985) 2909.
- [4] DENTON A. and ASHCROFT N. W., *Phys. Rev. A*, **39** (1989) 4701.
- [5] LINDEMANN F. A., *Phys. Z.*, **11** (1910) 609.
- [6] YOUNG D. A. and ALDER B. J., *J. Chem. Phys.*, **60** (1974) 1254.
- [7] BARKER J. A., *J. Chem. Phys.*, **63** (1975) 632.
- [8] LAIRD B. B., MCCOY J. D. and HAYMET A. D. J., *J. Chem. Phys.*, **87** (1987) 5449.
- [9] RAMAKRISHNAN T. V. and YUSSOUFF M., *Phys. Rev. B*, **19** (1979) 2775.
- [10] LÖWEN H., HANSEN J. P. and MADDEN P. A., *J. Chem. Phys.*, **98** (1993) 3275. For a recent general review on minimization methods, see: PAYNE M. C., TETER M. P., ALLAN D. C., ARIAS T. A. and JOANNOPOULOS J. D., *Rev. Mod. Phys.*, **64** (1992) 1045.
- [11] OXTOBY D. W., *Nature*, **347** (1990) 725, erroneously claimed that current density functional results exhibit the correct form of the anisotropy.
- [12] CURTIN W. A. and RUNGE K., *Phys. Rev. A*, **35** (1987) 4755.
- [13] PUSEY P. N., in *Liquids, Freezing and the Glass Transition*, edited by J. P. HANSEN, D. LEVESQUE and J. ZINN-JUSTIN (North-Holland, Amsterdam) 1991.
- [14] LEIDL R. and WAGNER H., *J. Chem. Phys.*, **98** (1993) 4142.